Comparison analysis based on different inverse algorithms of surface albedo products

QI Wendong[1,3], LIU Qiang[1,2], HONG Youtang[3]

1. *College of Global Change and Earth System Science, Beijing Normal University, Beijing* 100875, *China*;
2. *State Key Laboratory of Remote Sensing Science, Jointly Sponsored by Institute of Remote Sensing and Digital Earth, Chinese Academy of Sciences and Beijing Normal University, Beijing* 100101, *China*;
3. *School of Land Science and Technology, China University of Geosciences (Beijing), Beijing* 100083, *China*

Abstract: Surface albedo significantly affects the balance of surface energy and variation of global climate. Previously, surface a lbedo products have achieved significant success; however, many problems remain, such as low temporal resolution and missing data. Based on the observation data of uniform sites and MCD43B3 production of MODIS, this article verifies three algorithms and their products that arrive separately from a surface albedo production called Global LAnd Surface Satellite (GLASS): AB1 (ABD01), AB2(ABD03), and STF(ABD06). Then, we analyze and compare the improvement in quality between the initial and f inal products of GLASS. The result shows that the product ABD06 has the best matching with ground observation data, where the RMSE is 0 .050 and R^2 is 0.9. In addition, compared with MCD43B3's surface albedo product, the best consistency is also observed for ABD06, which is supported by the largest number of valid data among the three different products (ABD06 is 5507, ABD01 is 4290, and ABD03 is 3296), and the RMSE is better than 0.03, while R^2 is 0.9. Therefore, ABD06 is suitable for the production of long time series' surface albedo products. The statistical result for a large amount of data also shows that with up to 80% of the d ata coming from GLASS's three products, we can satisfy the accuracy requirement for the deviation between the climate model of the surface albedo and products (0.02—0.05).

Key words: surface albedo, MODIS, FLUXNET, time series, GLASS

CLC number: TP701 **Document code:** A

Citation format: **Qi W D, Liu Q and Hong Y T. 2014. Comparison analysis based on different inverse algorithms of surface albedo products. Journal of R emote Sensing, 1 8(3): 559 –572 [DOI: 10.11834/jrs.20143118]**

1 INTRODUCTION

The albedo is the diffuse reflectivity or reflecting power of a surface. It is defined as the ratio of the reflected radiation from the surface to the incident radiation arriving on it. The reflectance refers to the fraction of the reflected and incident solar radiation flux coming from the waveband of the surface. The albedo is the integration of all observed directions (Feng & Feng, 2012), and is not only an important factor for radiation fields, but is also an important parameter of the surface energy balance, mid-period and long-period weather prediction, and r esearch of global change which has extensive applications (Dickinson, et al., 1995; Wang, et al., 2011). The inversion of the albedo is meaningful to the study of the surface energy balance and atmospheric energy (Mason, et al., 2005).

Currently, numerous studies focusing on satellite remote sensing data for in-orbit operation and parts of airborne remote sensing data have been performed, and they also involved the valid ground verification of albedo production (Liang, et al., 2005; Liang, 2003; Lucht, et al., 2002; Russell, et al., 1997; Schaaf, et al., 2002; Jiao, et al., 2005; Wu, et al., 2012). The s urface bidirectional reflectance distribution function (BRDF)/a lgorithm of the albedo remote sensing inversion model based on the linear kernel drive model is currently the most popular method employed to realize surface albedo remote sensing inversion, and this method has been used in surface albedo production, such as MODIS and MISR. However, some problems still exist, although surface albedo production has u ndergone significant development. The main issues include: First, the comprehensive research and application of multisource data in surface albedo production are relatively less. Second, the use of a method that is based on bidirectional reflectance model inversion to calculate reflectance requires long periods to observe the data's inversion, leading to a low temporal resolution, which cannot reflect the rapid change of the albedo during rainfall, snowfalls, or plant growth. Third, recent algorithms are mainly

Received: 2013-05-09; **Accepted:** 2013-08-18; **Version of record first published:** 2013-08-25

Foundation: National High Technology Research and Development Program of China (No. 2009AA12210); National Natural Science Foundation of China (No. 41371356)

First author biography: QI Wendong (1987—), male, master candidate, he majors in 3s technique integration and application. E-mail: qiwendong2011@163.com

Corresponding author biography: HONG Youtang (1965—), male, associate professor, his main research interests are resources and environment remote sensing, remote sensing image processing and precision analysis. E-mail: Hongyoutang@163.com

directed at surfaces with plants. However, the accuracy of highly reflective ice and snow is not sufficient. Fourth, recent albedo production has been affected by cloud cover. Thus, numerous data are lost, and need to be supplemented. Fifth, the orographic influence, scale effect, and some other issues (Davidson, et al., 2004) related to the surface albedo are ignored in existing albedo inversion algorithms and running operations. In conclusion, by verifying the surface albedo production obtained by the Generation and Applications of Global Products E ssential Land Variables Project, this article estimates the surface albedo's reliability to provide scientific evidence for its subsequent production and application.

2 ALBEDO ALGORITHM AND PRODUCTION INTRODUCTION

2.1 Introduction of AMBRALS algorithm

NASA's moderate resolution imaging spectroradiometer (MODIS) team adopted algorithm for MODIS bidirectional r eflectance anisotropy of the land surface (AMBRALS) algorithm (Roujean, et al., 1992; Wanner, et al., 1995; Strahler, e t al., 1999), and then applied a semi-empirical model of a linear kernel driver to obtain global BRDF/Albedo production within a 1 km spatial discrimination by inversing the multi-angle and multiband MODIS observed data during a 16-day period (Schaaf, et al., 2002). The three steps involved in dealing with the algorithm include atmospheric correction, the modeling of the band reflectance angle, and albedo exchange from the narrowband to the broadband. This algorithm is based on the method of bidirectional reflection model inversion, and integrates the hemisphere space's Bidirectional Reflection Distribution Function (BRDF) model (Lucht, et al., 2002) so we can obtain a relatively accurate surface albedo inversion result (Yang, et al., 2002).

2.2 General framework of AB and STF algorithm

In this study, the remote sensing inversion of the surface a lbedo used the new algorithm angular bin (AB) (Qu, et al., 2013; Liang, et al., 2013). As a kind of direct inversion a lgorithm, this algorithm figures up a broadband surface albedo using a simple linear formula, and all information obtained by this algorithm comes from the multiband surface reflectivity or Top-of-Atmosphere (TOA) reflectivity. According to the different input data, the AB algorithm is divided into two sub-algorithms, AB1 and AB2 (Qu, et al., 2013), which calculate the black-sky and white-sky albedo of short waves (0.3—3 μm) based on the MODIS surface reflectance and TOA reflectivity, respectively. The characteristic of these two algorithms (AB1 and AB2) is such that it uses the input data of a single angle so that the output production's temporal resolution is high. In addition, the input data of the AB2 algorithm does not require atmospheric correction, therefore preventing the error due to the process of correcting the atmosphere MODIS data.

The surface parameter production of remote sensing inversion is always influenced by clouds, so there will be some missing data. The current approach to solving this problem is to combine several days' data of surface parameter production to r educe the ratio of missing data; however, this approach cannot completely eliminate this kind of deficiency. Considering this s ituation, the team researched a new algorithm named Statistics-based Temporal Filter (STF). This algorithm counts up the global surface albedo's background field of previously acquired knowledge based on MCD43, then fuses MCD43 products, AB1 and AB2 products, as well as smoothens and fills the lack of time s eries with the support of the background field (Fig. 1) (Liu, e t al., 2013).

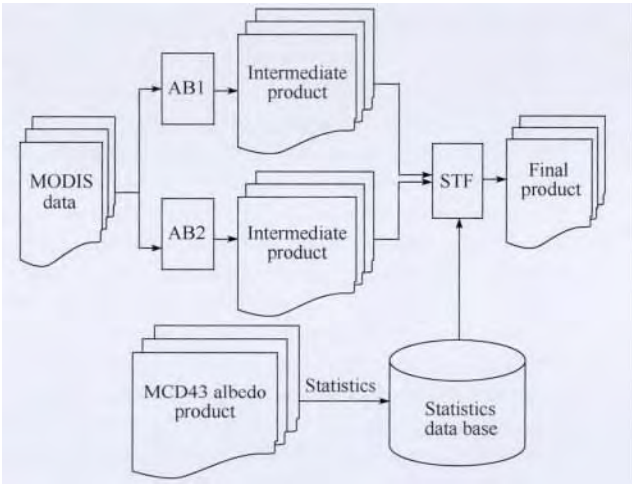

Fig. 1 Process flow sheet of albedo production GLASS

2.3 Production introduction

This article adopts ABD01 and ABD03 as the initial p roduction, and the purpose is to combine the final production ABD06. Compared with the initial production, ABD06 production generates more valid data resulting from the disposal of filtering and fusion. Therefore, it effectively reduces the negative influence of clouds, which leads to the phenomena of missing data. As expected, there is no doubt that the fusion process also causes data distortion in some cases. The product i nformation is shown in Table 1.

Table 1 Product information

Product name	Time resolution/d	Spatial resolution/km	Remark
ABD01	1	1	Product by AB1 algorithm
ABD03	1	1	Product by AB2 algorithm
ABD06	8	1	Product by STF algorithm
MCD43B3	8	1	Product by AMBRALS algorithm

Because MODIS production and GLASS production involve totally different algorithms, during the CLASS production, many initial and final productions have been simultaneously created because of different algorithms. Thus, it is necessary to analyze the characteristics of different generated data and to estimate the development of their quality for many initial and final produced data. This article analyzes and verifies these produced data based on observed data received from typical stations.

3 VALIDATION AND ANALYSIS

The quality of the final GLASS production relies on the a ccuracy of three algorithms: AB1, AB2, and STF. To test the actual effect of each algorithm, this article focuses on the c omparison analysis (which is based on different surface coverage types) between three kinds of GLASS production (GLASSABD) and real data coming from ground surface respectively. Then, we compared GLASSABD with MCD43B3. Finally, we analyze the comparison results because the ground test sites, ABD01 and ABD03, have a time resolution of 1 day. On the other hand, the time resolution of MCD43B3 and ABD06's is 8 days. Therefore, this article adopts 8 days as the u nified time resolution for the comparison and analysis of data. Based on this definition, data collected by ABD01, ABD03, and ground test sites should be reconstructed to match the 8-day time resolution. The substantial aggregation method is used to calculate the arithmetic average of the valid albedo rate data s elected among the times which are before and after 8 days (the total number of days is 16) of the specific time. If the valid data acquired in a 16-day period is less than 4, missing data can be determined.

3.1 Contrasting analysis between GLASSABD and ground observation data

AB1 and AB2 are based on the surface reflectivity and TOA reflectivity products, respectively, and we choose the data ABD01 and ABD03 from MODIS Terra's satellite, and filter the fusion products named ABD06 when compared with the ground observation data. According to the valid data of production, the time span is for data between 2006 and 2010. After selecting the ground test sites, we compared and analyzed the situation for d ifferent underlying surfaces: forest, grass and agriculture (Yu, 2009). The reason for neglecting the ground test sites having desert, ice and snow, frozen earth, and non-uniform coverage surfaces is because there are many problems associated with them, even though we have realized some development in these areas. These problems may include the presence of fewer models of these types of underlying surfaces, low model accuracy, and fewer ground test sites, which cannot guarantee the data's accuracy. In addition, we consider that there is an inconsistency between satellite pixels and the ground observation scale. Therefore, as much as possible, we selected ground test sites, which satisfied well-proportioned land cover and had plants as the u nderlying surface. In this way, we tested and verified the result of albedo remote sensing inversion, which may maximize verification's accuracy.

3.1.1 The selection of ground observed sites

The spatial scale for ground observation differs greatly from that of satellite remote sensing. If we directly compare surface observation data with remote sensing inversion data, many errors would be produced, which may affect the reliability of the results. Therefore, when we compare these produced data, the key factor is the selection of ground observation sites. The basic principle regarding their selection is to reduce the spatial scale influence produced by points affecting pixels. There are therefore two main factors: (1) the uniformity of the round surface sites. (2) whether or not the underlying surface of the observation sites have the same type as the main sites.

According to the principle of the selected site and the method selected by Cescatti, et al., (2012) (based on the manual of the albedo algorithm enacted by 863 projects), this article downloaded the higher resolution ratio image from surrounding sites, as in Fig. 2. Through visual interpretation to judge the s urface u niformity around sites, we can separate them into A, B, C, and D levels: the A level represents the best uniformity and the D level represents the worst uniformity. This manual collects the difference between the observed albedo for the non-snow condition and the published albedo production MCD43B3. If the root-mean-square-error is larger than 0.05, this site is unavailable. Therefore, we followed the standard that the difference of the root-mean-square-error between the ground observed data and MCD43B3 was less than 0.05; all of the data were selected in the A and B levels. Then, we selected as testing sites 24 sites that have the same type of underlying surface as that of the main site. The distribution of these sites can be seen in Fig. 3, and the basic information of the sites can be seen in Table 2.

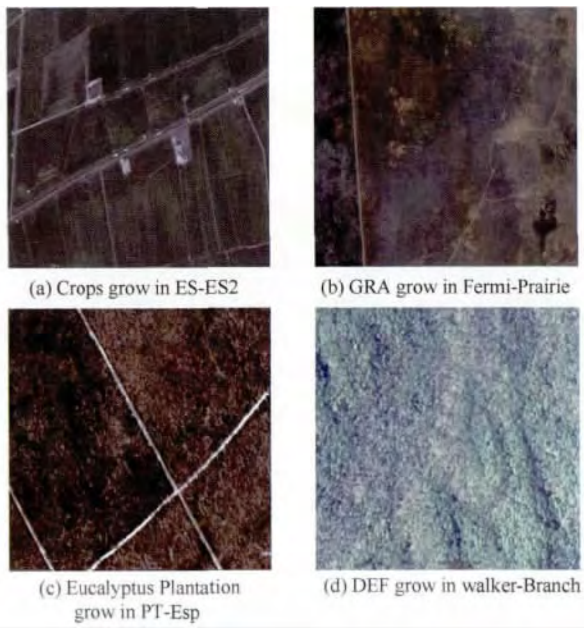

Fig. 2 Google Earth™ images used to assess the surface uniformity of the site

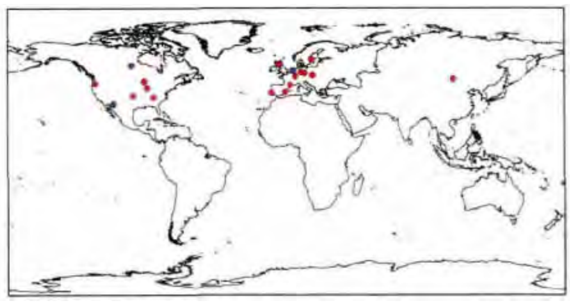

Fig. 3 Distribution of the 24 sites (Blue points mean more than one point)

Table 2 Basic information of ground observation site

Name	Latitude	Longitude	Surface coverage type	Name	Latitude	Longitude	Surface coverage type
ARM_SGP_Main	36.6050	-97.4884	CRO	DE-Hai	51.0793	10.4520	Beech
Audubon_Grassland	31.5907	-110.5100	GRA	DE-Kli	50.8929	13.5225	Crop
Fermi_Prairie	41.8406	-88.2410	GRA	DE-Tha	50.9636	13.5669	Spruce
Kendall_Grassland	31.7365	-109.9420	GRA	ES-ES2	39.2756	-0.3153	Crop
UCI_1850	55.8792	-98.4839	ENF	FR-Hes	48.6742	7.0656	Beech
UCI_1930	55.9058	-98.5247	ENF	FR-Pue	43.7414	3.5958	Oak
UCI_1964	55.9117	-98.3822	ENF	NL-Ca1	51.9710	4.9270	Grasslands
Walker_Branch	35.9588	-84.2874	DBF	NL-Loo	52.1679	5.7440	Scots pine
Willow_Creek	45.8059	-90.0799	DBF	PT-Esp	38.6398	-8.6018	Eucalyptus plantation
KBU	47.2140	108.7373	Uniform grassland	SE-Nor	60.0865	17.4795	Scots pine
CZ-BK1	49.5047	18.5411	Coniferous forest	UK-Gri	56.6072	-3.7981	Sitka spruce
Metolius_Intermediate_Pine	44.4524	-121.5570	ENF	DE-Geb	51.1001	10.9143	Crop

3.1.2 Comparison and analysis

Table 4 shows the data that was used in this paper. Fig. 4—Fig. 6 provide a comparison between ground observed data and GLASSABD data based on different underlying surfaces at 24 sites from 2006 to 2010.

Table 3 Introduction of the data used

Surface coverage type	Number of sites	Number of ABD01	Number of ABD03	Number of ABD06	Number of ground measured albedo	Timeframe of the data
Forest	15	2712	2395	3445	1105	2006—2010
Grassland	5	912	661	1103	717	2006—2010
Crop	4	708	556	920	608	2006—2010

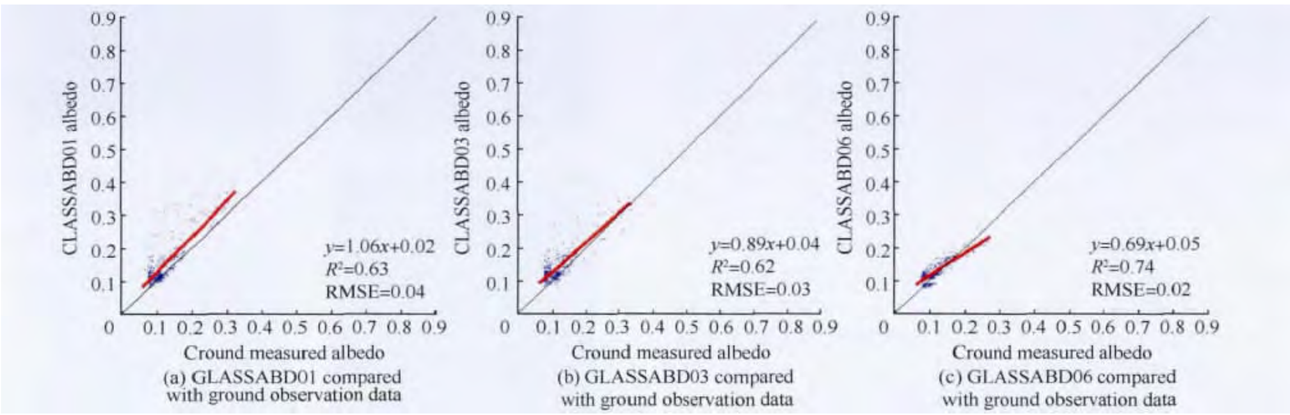

Fig. 4 GLASSABD compared with ground observation data based on the surface of underlying surface for forest

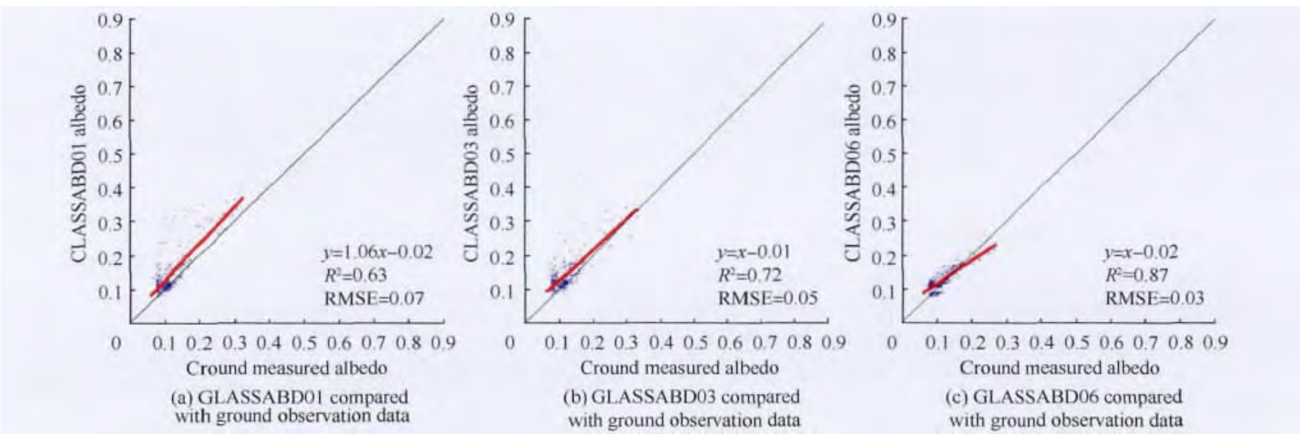

Fig. 5 GLASSABD compared with ground observation data based on the surface of underlying surface for grassland

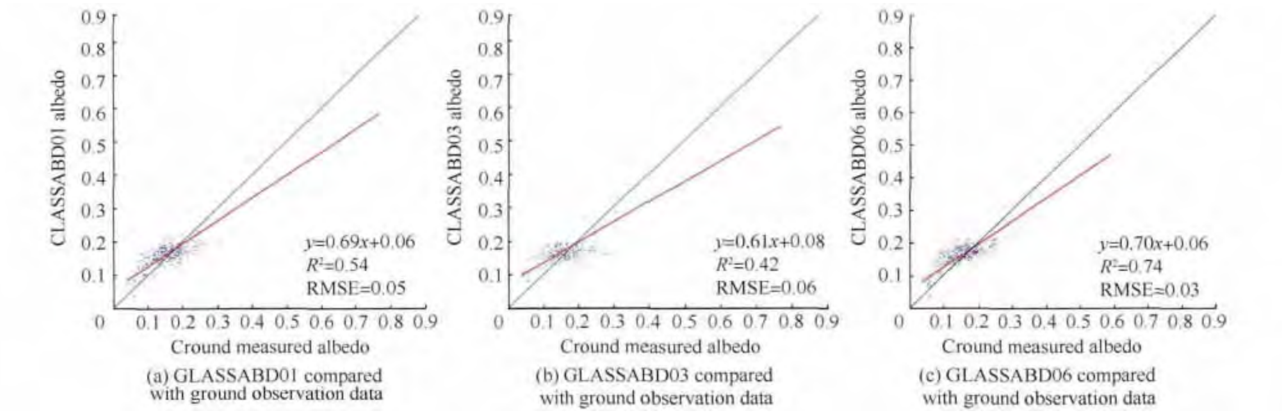

Fig. 6 GLASSABD compared with ground observation data based on the surface of underlying surface for crop

From the above comparison, we found that compared with ABD01 and ABD03, ABD06 and ground observed data had the highest fitting degree. In addition, ABD06 almost did not lose any data. All of these advantages indicated the superiority of the STF algorithm. However, since the STF algorithm still requires filtering and fusion, this process may leads to some data distortion. However, to some extent, AB1 and AB2 algorithms also match with ground observed data, which can be used as initial input data. On the other hand, compared with the use of agriculture as an underlying surface, data acquired by using forest and grass as the underlying surface is closer to the ground observed data. This is because the albedo in forests and grass is relatively stable. On the other hand, the growth period of agriculture is shorter, so the change rate of the albedo is higher; in addition, there will be a significant error due to averaging the albedo after the crops are reaped. Therefore, the fit between agriculture data and ground observed data is not good.

All of the analyses are based on the scatter diagram to compare the quality of data. Now, this article uses time series curve data to compare GLASSABD and the ground observed data. F ig. 2 provides a 1 km^2 Google Earth™ image of the site E S-ES2. From the figure, we observe that this area is a broad plain, which may be a good representation of agricultural ground cover. The geographic coordinates are (39.28°N, 0.32°W), and it is located in Spain. This area belongs to the Mediterranean type of subtropical zone climate, the summer is dry and hot, the winter is mild and rainy, and all of the summer and winter plants present are harvested two or three times annually. All of these are typical characteristics of subtropical agriculture. Fig. 7 is the time series figure of GLASSABD and ground observed data from 2006 to 2008 at the ES-ES2 site. According to this figure, this site only has three years worth of data, spanning 2006 to 2008. In addition, some data are missing. However, no data are missing from the 5-year albedo production period of ABD06, so it can better reflect the agricultural growth period and changing tendency of albedo. This site is located at a place in which plants are usually harvested twice annually. The ground albedo in spring and fall is larger compared with that in summer. This is because the humidity is lower during spring and fall. Davidson, et al., (2004), pointed out that the ground albedo will decrease when the soil humidity increases. Further, this change is much more obvious when the soil contain less water. In the spring, the chlorophyll in plants is reduced during harvesting of agricultural crops; at the same time, the moisture content is lower and the ground albedo is higher. During reaping, the value of the albedo reaches its the maximum annual value. Then, during the process of replanting, germinating and growing, the ground albedo will be reduced. When agricultural crops thrive throughout the entire year, the soil moisture content is higher and the ground albedo is lower. ABD06 production expresses this process very well, and the data is relatively consistent with ground observed data. Fig. 4 shows the comparison result that does not differentiate between the underlying surface of GLASSABD and ground observed d ata.

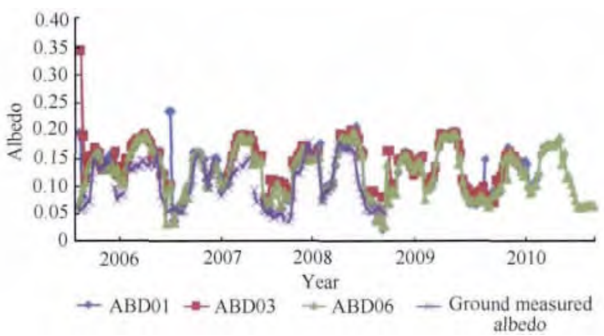

Fig. 7 The time sequence diagram for GLASSABD compared with ground observation data in ES-ES2 from 2006 to 2010

Table 4 Results of GLASSABD compared with ground observation data

Data type	The amount of data	Bias	RMSE	R^2
ABD01	4290	0.007	0.056	0.602
ABD03	3296	0.004	0.052	0.526
ABD06	5507	0.001	0.050	0.788

3.2 Contrasting analysis between GLASSABD and MCD43B3

Because the MCD43B3's time resolution from NASA is also eight days, the data processing is the same as when GLASSABD is compared with MCD43B3 and when compared with the ground observation data. The only difference is that it generally refers to the underlying surface as plants rather than subdividing the underlying surface from the plant.

3.2.1 Comparison between MCD43B3 and all kinds of statistics data of production

When compared with MCD43B3, this article still used the data from the above-mentioned 24 sites, which were acquired b etween 2006 and 2010. In this paper, we collected 4290 ABD01 data, 3296ABD03 data, 5507ABD06 data, and 4696MCD43B3 data. It can be seen that ABD06 had almost no data loss, while MCD43B3 missed more data. ABD06 is more suitable than MCD43B3 in the time sequence only, while the data is considered to be effective. Fig. 8 shows the comparison between GLASSABD and MCD43B3.

When comparing with MCD43B3, we still used the data from the above-mentioned 24 sites for the time span 2006 to 2010. In this paper, we collected 4290 sets of ABD01 data, 3296 sets of ABD03 data, 5507 sets of ABD06 data, and 4696 sets of MCD43B3 data. It can be seen that ABD06 had almost no data loss, while MCD43B3 was missing more data. ABD06 is more suitable than MCD43B3 in time sequence, only consider the data effectively. Fig. 8 shows the comparison of GLASSABD and MCD43B3.

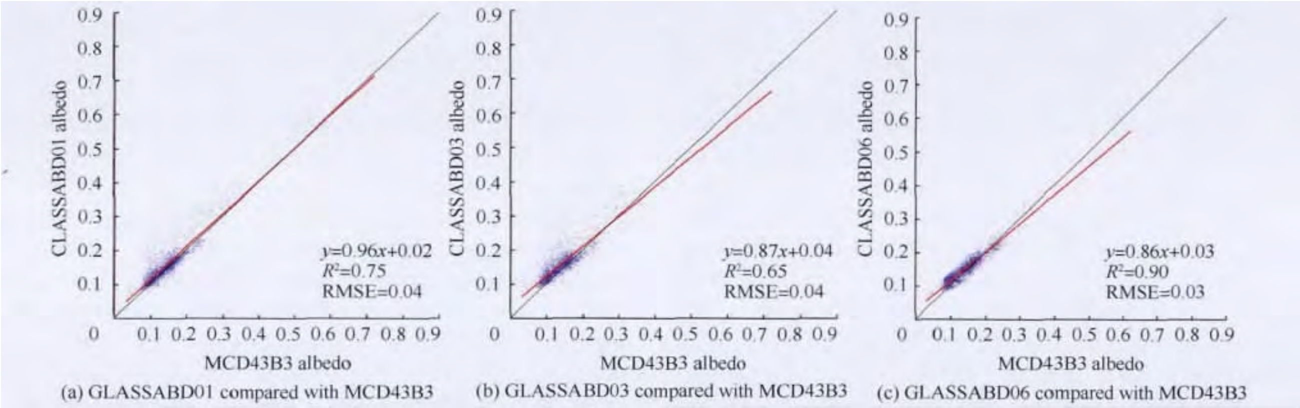

Fig. 8 GLASSABD compared with MCD43B3

3.2.2 Results and analysis

Considering the result of the comparison for all albedo p roduction of AhBD01, AND03, and ABD06 based on various vegetation types and MCD43B3 albedo product, the ABD06 was found to be the most consistent with MCD43B3, ABD01, ABD03, and MCD43B3 all having data loss, while there are some mutational points that do not agree well with MCD43B3. The residual error of the atmospheric correction inside the ABD01 and ABD03 may be attributed to the deviation of the MODIS pixel geometric position on different dated and the u ncertainty of the algorithms themselves. It is also possible that these mutant points fit the real situation; however, they are eliminated through fusion filtering by inputting data using STF algorithms. Therefore, we require more prior knowledge during the production process. We find that the value of ABD06 is slightly higher than that of MCD43B3 after a long validation sequence. Compared with ABD01 and ABD03, ABD06 is closer to MCD43B3,but ABD01 and ABD03 also had the desired effect. The STF algorithm is more suitable for producing a long albedo time series. Table 5 is a summary of the GLASSABD results compared with those of MCD43B3.

Table 5 Results of GLASSABD compared with MCD43B3

Data type	The amount of data	Bias	RMSE	R^2
ABD01	4290	0.12	0.04	0.75
ABD03	3296	0.13	0.04	0.65
ABD06	5507	0.007	0.03	0.90

4 CONCLUSION

To quantitatively validate the quality of Land-surface albedo products for three types of algorithms (AB1, AB2, and STF), we selected 24 ground observation sites, and compared AB1, AB2, STF and MCD43B3 with relevant ground observation data. The scope of the data was limited from 2006 to 2010. Based on large amounts of data, the statistical results show that AB1and AB2 a chieved the desired effect, and can satisfy the accuracy requirement (compared with the ground observation site data, R2 is b etter than 0.5, and the RMSE is about 0.05; compared with MCD43B3, R^2 is better than 0.65, and the RMSE is better than 0.04). As a filtering and fusion product, the albedo produced by STF has more effective data, and this production has a continuous time sequence, and the albedo change is stable. We found that the STF algorithm had certain advantages. Compared with the ground observation data, the STF algorithm has the best fit, and the bias is close to 0.001. The RMSE is better than 0.05 and R^2 is close to 0.8. Compared with MCD43B3, ABD06 p roduced by the STF algorithm has the best fit, and the bias is better than 0.007, The RMSE is close to 0.03, and R^2 is better than 0.9. Numerous validated results also indicated that all the deviations obtained from a comparison of over 80% of the data for three types of GLASS production and ground observation data could satisfy the accuracy requirements within the scope of 0.02—0.05 in the climatic patterns (Henderson-Sellers, et al., 1983; Sellers, et al., 1993). However, AB1 and AB2 have a problem regarding missing data when affected by clouds, so the albedo production obtained by STF may be more suitable as the input data when we carry out research into global changes.

Many problems, such as the poor quality of the data p roduced by AB1 and AB2 algorithms and the generation of large amounts of missing data, may be attributed to a residual e rror of atmospheric correction, the deviation of the MODIS pixel geometric position on different dates, and the uncertainty of AB1 and AB2 algorithms. Meanwhile, the STF algorithm also has some defects, such as the fact that filtering fusion is likely to filter out some points which correspond to the actual situation, but beating larger. Li et al., 1995 emphasized the importance of obtaining prior knowledge in remote sensing inversion. To obtain a higher accuracy of inversion values, we need to introduce more prior knowledge.

REFERENCES

Cescatti A, Marcolla B, Santhana Vannan S K, Pan J Y, Román M O, Yang X Y, Ciais P, Cook R B, Law B E and Matteucci G, Migliavacca M, Moors E, Richardson A D, Seufert G and Schaaf C B. 2012. Intercomparison of MODIS albedo retrievals and in situ measurements across the global FLUXNET network. Remote Sensing of Environment, 121: 323 – 334 [DOI: 10.1016/j.rse.2012.02.019]

Davidson A and Wang S S. 2004. The effects of sampling resolution on the surface albedos of dominant land cover types in the North A merican boreal region. Remote Sensing of Environment, 93(1/2): 211 – 224 [DOI: 10.1016/j.rse.2004.07.005]

Dickinson R E. 1995. Land processes in climate models. Remote Sensing of Environment, 51(1): 27 – 38 [DOI: 10.1016/0034 – 4257(94)00062 – R]

Feng Y and Feng H X. 2012. TM data retrieval and analysis of Beijing area surface albedo. Science of Surveying and Mapping, 37(5): 164 – 166

Henderson-Sellers A and Wilson M F. 1983. Surface albedo data for climatic modeling. Reviews of Geophysics, 21(8): 1743 – 1778 [DOI: 10.1029/RG021i008p01743]

Jiao Z T, Wang J D, Xie L O, Zhang Y, Yan G J, He L M and Li X W. 2005. Initial validation of mODIS albedo product by using field Measurements and Airborne Multiangular Remote Sensing Observations. Journal of Remote Sensing, 9(1): 64 – 72

Li X W, Wang J D and Strahler A H. 1995. On utilization of a *priori* knowledge in inversion of remote sensing models. Science in China Series D (Earth Sciences), 41(6): 580 – 585 [DOI: 10.1007/BF02878739]

Liang S L. 2003. A direct algorithm for estimating land surface broadband albedos from MODIS imagery. IEEE Transactions on Geoscience and Remote Sensing, 41(1): 136 – 145 [DOI: 10.1109/TGRS.2002.807751]

Liang S L, Stroeve J and Box J E. 2005. Mapping daily snow/ice shortwave broadband albedo from Moderate Resolution Imaging Spectroradiometer (MODIS): the improved direct retrieval algorithm and validation with Greenland in situ measurement. Journal of Geophysical Research, 110(D10) [DOI: 10.1029/2004JD005493]

Liang S L, Zhao X, Liu S H, Yuan W P, Cheng X, Xiao Z Q, Zhang X T, Liu Q, Cheng J, Tang H R, Qu Y H, Bo Y C, Qu Y, Ren H Z, Yu K and Townshend J. 2013. A Long-term Global LAnd Surface Satellite (GLASS) data-set for environmental studies. International Journal of Digital Earth, [DOI: 10.1080/17538947.2013.805262]

Liu N F, Liu Q, Wang L Z, Liang S L, Wen J G, Qu Y and Liu S H. 2004. A statistics-based temporal filter algorithm to map spatiotemporally continuous shortwave albedo from MODIS data. Hydrology and Earth System Sciences, 17: 2121 – 2129 [DOI: 10.5194/hess – 17 – 2121 – 2013]

Lucht W, Schaaf C B and Strahler A H. 2002. An algorithm for the retrieval of albedo from space using semiempirical BRDF models. IEEE Transactions on Geoscience and Remote Sensing, 38(2): 977 – 998 [DOI: 10.1109/36.841980]

Mason P and Reading B. 2005. Implementation Plan for the Global Observing System for Climate in Support of the UNFCCC. Geneva, Switzerland: WMO, IOC, UNEP, ICSU

Qu Y, Liu Q, Liang S, Wang L Z, Liu N F and Liu S H. 2013. Direct-estimation algorithm for mapping daily land-surface broadband albedo from MODIS data. IEEE Transactions on Geoscience and Re mote Sensing, (99): 1 [DOI: 10.1109/TGRS.2013.2245670]

Roujean J L, Leroy M and Deschamps P Y. 1992. A bidirectional reflectance model of the Earth's surface for the correction of remote sensing data. Journal of Geophysical Research, 97(D18): 20455 – 20468 [DOI: 10.1029/92JD01411]

Russell M J, Nunez M, Chladil M A, Valiente J A and Lopez-Baeza E. 1997. Conversion of nadir, narrowband reflectance in red and near-infrared channels to hemispherical surface albedo. Remote Sensing of Environment, 61(1): 16 – 23 [DOI: 10.1016/S0034 – 4257(96)00218 – 0]

Schaaf C B, Gao F, Strahler A H, Lucht W, Li X W, Tsang T, Strugnell N C, Zhang X Y, Jin Y F, Muller J P, Lewis P, Barnsley M J, Hobson P, Disney M, Roberts G, Dunderdale M, Doll C, D'Entremont R P, Hu B X, Liang S L, Privette J L and Roy D. 2002. First operational BRDF, albedo nadir reflectance products from MODIS. Remote Sensing of Environment, 83(1/2): 135 – 148 [DOI: 10.1016/s0034 – 4257(02)00091 – 3]

Sellers P J. 1993. Remote Sensing of Land Surface Climatology. NASA/GSFC Intematiorlal Satellite Land Surface C1inlatology Project Report. Greenbelt, Maryland: NASA Goddard Space Flight Center

Strahler A H, Lucht W, Schaaf C B, Tsang T, Gao F, Li X W, Muller J P, Lewis P and Barnsley M. 1999. MODIS BRDF/albedo product: algorithm theoretical basis document version 5.0. MODIS documentation

Wang Y, Zhu B, Liu Y and Li W L. 2011. Trend of surface albedo changes in China in last decade. Meteorological Science and Technology, 39(2): 147 – 155

Wanner W, Li X and Strahler A. 1995. On the derivation of kernels for kernel-driven models of bidirectional reflectance. Journal of Geophysical Research, 100(D10): 21077 – 21090 [DOI: 10.1029/95JD02371]

Wu H Y, Tong L and Chen Y P. 2012. Evaluation of MODIS shortwave albedo products over ChinaFLUX sites. Remote Sensing Technology and Application, 27(5): 735 – 739

Yang H, Li X W and Gao F. 2002. An algorithm for the retrieval of albedo from space using new go kernel-driven BRDF model. Journal of Remote Sensing, 6(4): 246 – 251

Yu Y, Li Y Y, Tong Y X, Tian H and Chen H B. 2009. Observation and analysis of surface albedo of wheat and rice fields in Shouxian region. Climatic and Environmental Research, 14(6): 639 – 645

3 种反演算法的地表反照率遥感产品对比分析

齐文栋[1,3]，刘强[1,2]，洪友堂[3]

1. 北京师范大学 全球变化与地球系统科学学院，北京 100875；
2. 遥感科学国家重点实验室 中国科学院遥感与数字地球研究所，北京 100101；
3. 中国地质大学(北京) 土地科学技术学院，北京 100083

摘 要:地表反照率对于地表能量平衡和全球气候变化具有重要的影响。近年来,地表反照率产品已经取得了较为广泛的应用,但是仍存在时间分辨率低和数据缺失等问题。本文基于均匀站点观测数据与 MODIS 的 MCD43B3 产品验证了 GLASS (Global LAnd Surface Satellite)地表反照率产品的 3 种算法及其对应的反照率产品:AB1(ABD01)、AB2(ABD03)和 STF(ABD06)。并分析比较了 GLASS 反照率初级产品到最终产品的质量提升。结果表明:最终产品 ABD06 与地面观测数据符合最好,RMSE 为 0.050，R^2 为 0.788;同时,ABD06 与 MCD43B3 反照率产品一致性最好，RMSE 优于 0.03,R^2 达到 0.9,且 ABD06 有效数据最多(ABD01 为 4290,ABD03 为 3296,ABD06 为 5507),比较适合生产长时间序列的反照率产品。大量数据的统计结果还表明:3 种 GLASS 产品 80% 以上的数据与地面观测数据的偏差均能满足气候模式对反照率的精度要求(0.02—0.05)。

关键词:地表反照率,MODIS,FLUXNET,时间序列,GLASS

中图分类号:TP701 文献标志码:A

引用格式:齐文栋,刘强,洪友堂.2014.3 种反演算法的地表反照率遥感产品对比分析.遥感学报,18(3):559－572

Qi W D, Liu Q and Hong Y T. 2014. Comparison analysis based on different inverse algorithms of surface albedo products. Journal of Remote Sensing, 18(3):559－572 [DOI: 10.11834/jrs.20133118]

1 引 言

地表反照率 Albedo 指地表对入射的太阳辐射的反射通量与入射的太阳辐射通量的比值,而地表对某波段在一定方向上反射的太阳辐射通量与入射太阳辐射通量之比,称为地表反射率,反照率是反射率对所有观测方向的积分(冯淼和冯海霞,2012)。地表反照率既是地面辐射场的重要要素之一,也是一个广泛应用于地表能量平衡、中长期天气预测和全球变化研究的重要参数(Dickinson,1995;王艺等,2011)。地表反照率的反演对于地表能量平衡和大气能量等的研究具有重要的意义(Mason 和 Reading,2005)。

学者针对在轨运行的卫星遥感数据以及部分航空遥感数据进行大量地表反照率反演研究,并进行了有效的反照率产品的地面验证(Liang 等,2005;Liang,2003;Lucht 等,2002;Russell 等,1997;Schaaf 等,2002;焦子锑 等,2005;吴宏伊 等,2012),其中基于线性核驱动模型的地表 BRDF/反照率遥感反演模型算法是目前地表反照率遥感反演中应用最广泛的方法,已经在 MODIS、MISR 的地表反照率产品中得到了很好的应用。虽然地表反照率产品的生成已经取得了巨大的进展,但是仍然存在着一些问题:(1)目前地表反照率产品综合利用多源数据的研究和应用很少;(2)基于二向反射模型反演方法计算反照率需要较长周期的观测数据进行反演,因此时间分辨率低,不能反映雨雪或者植被快速生长过程中地表反照率的快速变化;(3)目前算法主要针对植被地表,对于冰雪等高反射地表精度不高;(4)目前的反照率产品受云的影响,数据缺失较多,需要进行填补;(5)地表反照率的地形影响、尺度效应(Davidson和 Wang,2004)等问题都在现有的业务化

收稿日期:2013-05-09;修订日期:2013-08-18;优先数字出版日期:2013-08-25
基金项目:国家高技术研究发展计划(863 计划)(编号:2009AA12210);国家自然科学基金(编号:41371356)
第一作者简介:齐文栋(1987—),男,硕士研究生,现从事 3S 技术集成与应用研究。E-mail:qiwendong2011@163.com
通信作者简介:洪友堂(1965—),男,副教授,主要从事摄影测量与遥感方面研究。E-mail:Hongyoutang@163.com

运行的反照率反演算法中被忽略。本文通过验证最新 863 计划“全球陆表特征参量产品生成与应用研究”生产的地表反照率产品，对最终的地表反照率可靠度进行评价，为后续的生产与应用提供科学依据。

2 反照率算法和产品简介

2.1 AMBRALS 算法介绍

NASA MODIS 科学团队采用 AMBRALS（Algorithm for MODIS Bidirectional Reflectance Anisotropy of the Land Surface）算法（Roujean 等，1992；Wanner 和 Strahler，1995；Strahler 等，1999），应用半经验的线性核驱动模型，对 16 天周期的多角度多波段 MODIS 观测数据反演得到 1 km 空间分辨的全球 BRDF/Albedo 产品（Schaaf 等，2002），算法的处理流程主要包括大气校正、波段反射率的角度建模以及窄波段向宽波段反照率转换 3 个步骤。该算法是基于二向反射模型反演的方法，在半球空间上对 BRDF（Bidirectional Reflectance Distribution Function）模型（Lucht 等，2002）进行数值积分，可以得到较为精确的地表反照率反演结果（杨华 等，2002）。

2.2 AB、STF 算法总体框架

在本研究中，地表反照率的遥感反演使用了国家 863 计划“全球陆表特征参量产品生成与应用研究”项目组新研发的 Angular Bin 算法（简称 AB 算法）（Qu 等，2013；Liang 等，2013）。该算法作为一种直接反演算法，直接从多波段的地表方向反射率或者大气层顶方向反射率中通过简单的线性公式计算出宽波段地表反照率。根据输入数据的不同，AB 算法又分为 AB1 和 AB2 两个子算法（Qu 等，2013），他们分别基于 MODIS 地表反射率和大气层顶反射率数据计算短波（0.3—3 μm）波段的黑空反照率和白空反照率。AB1 算法和 AB2 算法的特点是仅使用单一角度的输入数据，因此输出产品的时间分辨率高；另外，AB2 算法的输入数据无需做大气校正，因此回避了 MODIS 数据大气校正过程中可能引入的误差。

遥感反演的地表参数产品都会受到云的影响而出现数据缺失现象，目前多数地表参数产品通过多天（如 8 天、16 天）数据合成在一定程度上减少缺失数据的比例，但是并不能彻底消除缺失。因此项目组提出了地表反照率时间序列的平滑和缺失填补算法（简称 STF 算法），首先根据 NASA 发布的 MODIS 地表反照率产品（MCD43）统计全球地表反照率先验知识背景场，然后在背景场支持下进行 MCD43 产品、AB1 产品和 AB2 产品的融合以及时间序列平滑和缺失填补（图 1）（Liu 等，2013）。

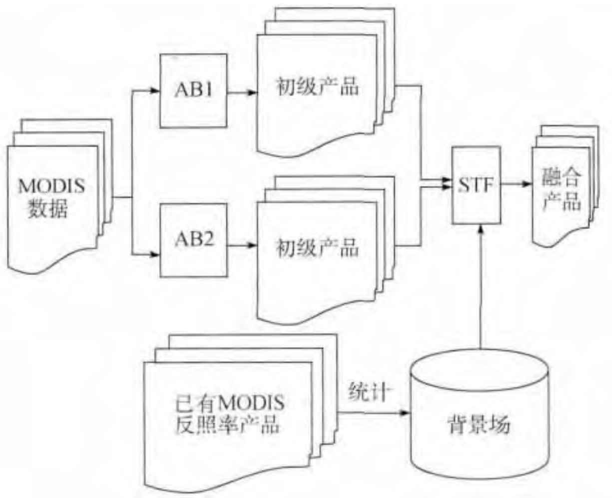

图 1　GLASS 反照率产品的生产流程图

2.3 产品介绍

文中的 ABD01 与 ABD03 为初级产品，目的是合成最终产品 ABD06，相比初级产品，ABD06 产品经过融合滤波处理后有效数据明显增多，有效地减少了受云影响导致数据缺失的现象，但是融合的过程中也会导致部分数据失真（表 1）。

表 1　产品信息表

产品名称	时间分辨率/天	空间分辨率/km	备注
ABD01	1	1	用 AB1 算法生产
ABD03	1	1	用 AB2 算法生产
ABD06	8	1	用 STF 算法生产
MCD43B3	8	1	用 AMBRALS 算法生产

因为 MODIS 产品和 GLASS 产品具有完全不同的算法，而且 GLASS 产品在生产过程中又由不同的算法生成了多种初级产品和最终产品，所以有必要分析不同算法生成的产品的特点，并对 GLASS 产品在生产过程中初级产品到最终产品质量的提升进行评价。本文基于典型站点观测数据对这些产品进行了分析和验证。

3 验证分析

GLASS 最终产品的质量依赖于 AB1、AB2 和 STF 3 个算法的精度,为验证各种算法的实际效果,用 3 种 GLASS 产品(以下简称 GLASSABD)与地面实测数据基于不同的下垫面覆盖类型进行了对比分析,并与 MCD43B3 进行对比,最后分析对比结果。由于地面验证站点与 ABD01、ABD03 的时间分辨率为 1 天,而 MCD43B3 与 ABD06 的时间分辨率为 8 天,因此文中统一采用时间分辨率为 8 天的数据进行比较,这就需要将 ABD01、ABD03 以及地面验证站点数据的时间分辨率聚合成每 8 天,聚合方法为对特定时间的前后各 8 天共 16 天内有效的反照率数据进行算数平均,如果 16 天内的有效数据少于 4 个,则认为数据缺失。

3.1 GLASSABD 与地面观测数据的对比分析

AB1、AB2 为分别基于地表反射率和大气层顶反射率的反照率产品,在与地面观测数据对比时选用的是 MODIS Terra 卫星数据产品 ABD01/ABD03 和滤波融合产品 ABD06。时间跨度根据各种产品的有效数据,主要为 2006 年—2010 年的数据。在选定地面验证站点的基础上文中分别基于森林、草地和农作物 3 种下垫面进行对比分析(余予 等,2009)。文中没有选取下垫面为沙漠、冰雪、冻土以及非均匀覆盖的地面验证站点,原因是尽管这些区域的地表反照率在之前的研究中取得了一定进展,但是尚有较多的问题,例如针对这些下垫面的模型较少,模型精度相对较低,地面验证站点较少,精度无法保证,再考虑到卫星像元与地面观测尺度不一致的问题,因此尽量选取了地表覆盖较为均匀且下垫面为植被的地面验证站点来验证反照率遥感反演结果,最大限度地保证验证的精度。

3.1.1 地面观测站点的选取

地面观测的空间尺度与卫星遥感的观测空间尺度存在巨大的差异,直接用地面观测数据与遥感反演数据进行对比会对结果产生一定的误差,影响结果可靠性,因此在地面观测数据与遥感反演产品比较时,地面观测站点的选取是关键,减小点对像元的空间尺度的影响是地面观测站点选取的基本原则。因此在对站点的筛选时主要考虑了两个因素:(1)观测站点地表周围是否均匀;(2)观测站点的下垫面是否与区域的主要下垫面一致。

文中参考了 863 计划制定的《反照率算法手册》中对观测站点筛选的原则和 Cescatti(Cescatti 等,2012)的筛选方法,下载了站点周边的较高分辨率影像(TM 影像和 Google Earth),如图 2。通过目视判读判断站点周边的地表均匀性,把站点分为 A、B、C 和 D 4 个级别,A 级站点表示均匀性最好,D 级表示均匀性最差。手册中统计了无雪条件下站点观测的反照率与 NASA 发布的反照率产品 MCD43B3 的差异,如果 RMSE 大于 0.05,则认为该站点不可用。因此我们根据站点均匀性为 A、B 级以及站点观测与 MCD43B3 产品 RMSE 不超过 0.05 为标准,从收集的台站观测数据中筛选了 24 个站点作为验证站点。这 24 个验证站点的下垫面与区域的主要下垫面类型一致。站点的分布如图 3,基本信息见表 2。

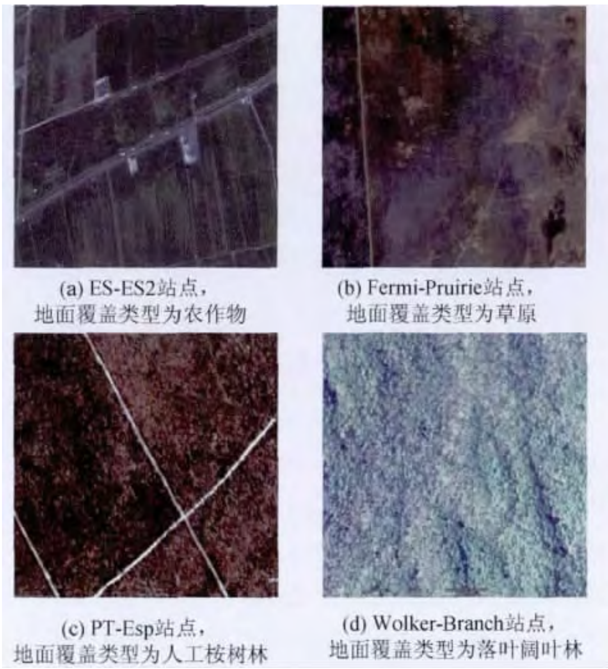

图 2 通过目视判断 Google Earth™ 高分辨率影像,判断 FLUXNET 站点的地表均匀性(影像覆盖范围为以地面观测站点为中心的 1 km² 区域)

图 3 24 个观测站点的全球分布图
(蓝色点为由于距离较近造成重叠的站点)

表 2 地面观测站点基本信息

站点名称	纬度	经度	地表覆盖类型	站点名称	纬度	经度	地表覆盖类型
ARM_SGP_Main	36.6050	-97.4884	农田	DE-Hai	51.0793	10.4520	榉木林
Audubon_Grassland	31.5907	-110.5100	草原	DE-Kli	50.8929	13.5225	农田
Fermi_Prairie	41.8406	-88.2410	草原	DE-Tha	50.9636	13.5669	云杉
Kendall_Grassland	31.7365	-109.9420	草原	ES-ES2	39.2756	-0.3153	农田
UCI_1850	55.8792	-98.4839	常绿针叶林	FR-Hes	48.6742	7.0656	榉木林
UCI_1930	55.9058	-98.5247	常绿针叶林	FR-Pue	43.7414	3.5958	橡木林
UCI_1964	55.9117	-98.3822	常绿针叶林	NL-Ca1	51.9710	4.9270	草原
Walker_Branch	35.9588	-84.2874	落叶阔叶林	NL-Loo	52.1679	5.7440	苏格兰松树林
Willow_Creek	45.8059	-90.0799	落叶阔叶林	PT-Esp	38.6398	-8.6018	人工桉树林
KBU	47.2140	108.7373	草原	SE-Nor	60.0865	17.4795	苏格兰松树林
CZ-BK1	49.5047	18.5411	针叶林	UK-Gri	56.6072	-3.7981	云杉
Metolius_Intermediate_Pine	44.4524	-121.5570	常绿针叶林	DE-Geb	51.1001	10.9143	农田

3.1.2 对比与分析

表 3 为文中使用数据说明，图 4—图 6 给出了 24 个站点在 2006 年—2010 年基于不同下垫面的地面观测数据与 GLASSABD 产品对比的散点图。

表 3 使用数据说明表

下垫面类型	站点数目	ABD01 数据量	ABD03 数据量	ABD06 数据量	地面观测数据	数据时间范围
森林	15	2712	2395	3445	1105	2006 年—2010 年
草地	5	912	661	1103	717	2006 年—2010 年
农作物	4	708	556	920	608	2006 年—2010 年

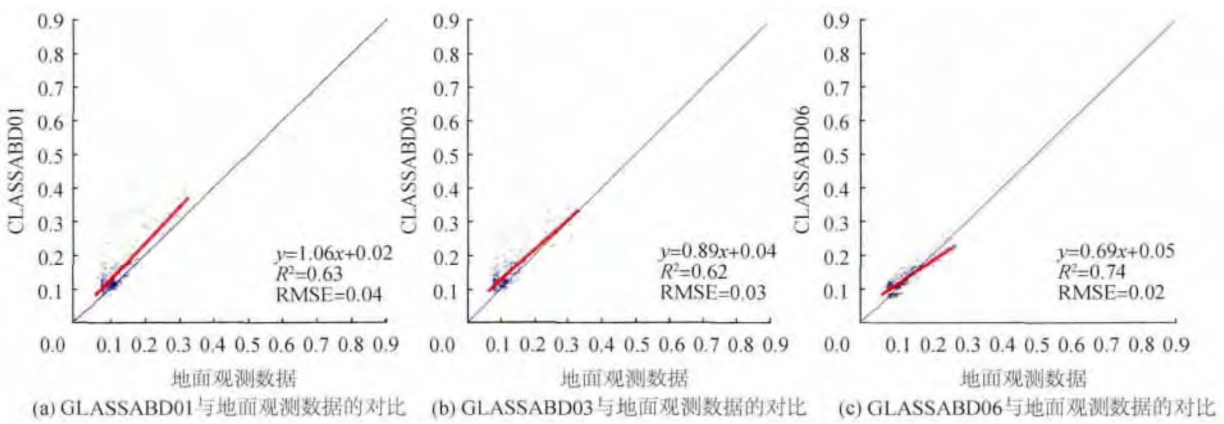

图 4 基于地表下垫面为森林的 GLASSABD 与地面观测数据的对比图

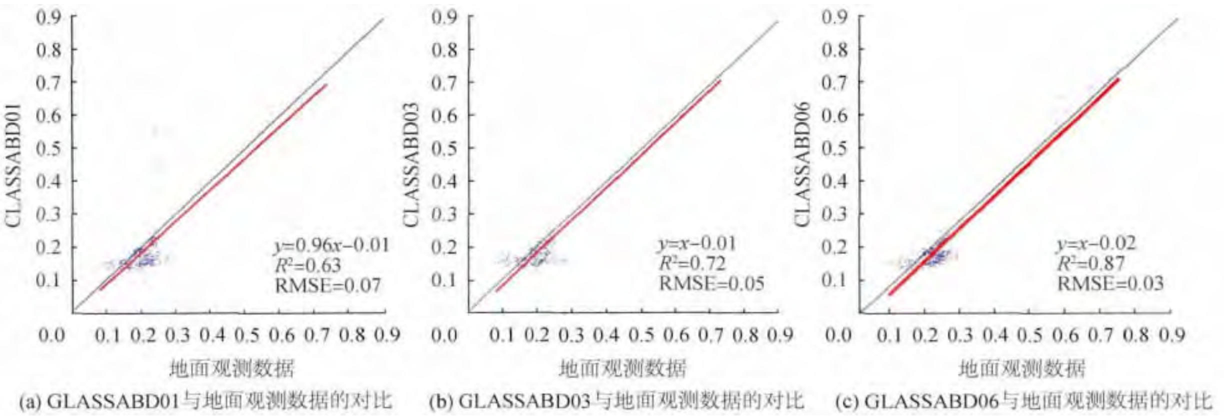

图 5 基于地表下垫面为草地的 GLASSABD 与地面观测数据的对比图

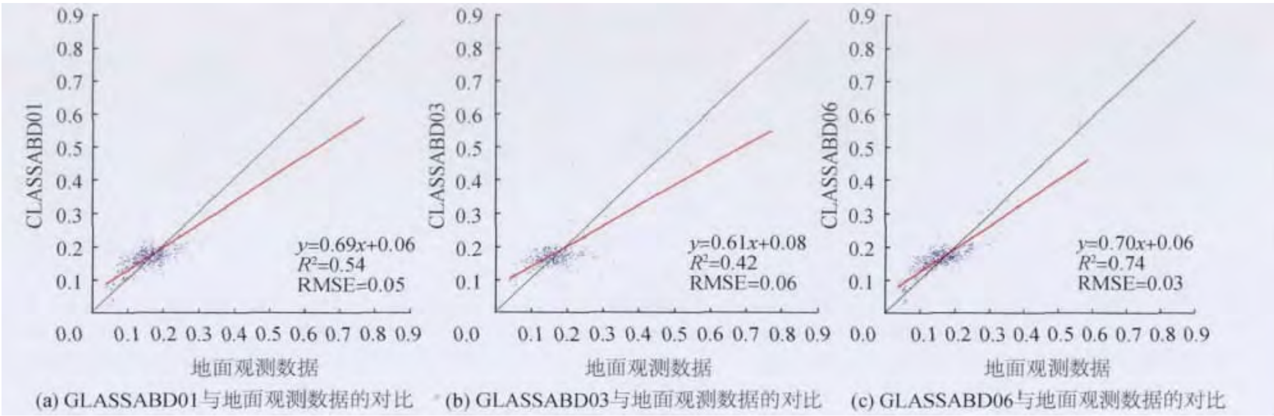

图6 基于地表下垫面为农作物的 GLASSABD 与地面观测数据的对比图

通过以上对比发现,相比于 ABD01 和 ABD03,ABD06 与地面观测数据的拟合程度最高,且 ABD06 产品几乎没有数据缺失,体现了 STF 算法的优越性,但由于 STF 算法需要进行滤波融合,这也可能导致 ABD06 部分数据的失真。AB1、AB2 算法与地面观测数据的值也比较吻合,可以作为最初的输入数据,达到了预期效果。相比地表下垫面为农作物,下垫面为森林和草地时 GLASSABD06 与地面观测数据更接近。这是由于森林和草地的反照率的值相对来说比较稳定,而农作物生长周期较短,地表反照率的值变化较大,再加上农作物的收割导致取平均值的过程中产生较大的误差,因此农作物整体上与地面观测数据的拟合较差。

以上都是通过散点图来比较数据的质量,下面我们通过时间序列曲线图来对 GLASSABD 与地面观测数据进行比较。图 2 给出了 Google Earth™ 在 ES-ES2 站点 1 km^2 区域影像,可以看出,ES-ES2 站点所在的地区为宽广的平原,为农作物地表覆盖类型,地表具有较好的代表性。站点地理坐标为(39.28°N,0.32°W),位于欧洲西南的伊比利亚半岛上的西班牙,东临地中海。属于地中海型亚热带气候,夏季炎热干燥,冬季温和多雨,有冷、热两季,冷季种喜凉作物,热季种喜温作物,喜凉和喜温不同生态型作物一年两熟或三熟,是亚热带农业的基本特征。图7 为 ES-ES2 站点 2006 年—2010 年 GLASSABD 与地面观测数据的时间序列图,由图 7 可知,在这个站点,地面观测数据只有 2006 年—2008 年 3 年的数据,并且这 3 年中有数据缺失情况。相比之下,ABD06 反照率产品 5 年内没有数据缺失情况,因此可以更好地反映农作物的生长周期与反照率的变化趋势。该站点所处位置农作物为一年两熟,地表反照率在春秋季节较大,在夏季较小,这是由于春秋季节土壤湿度较小。Davidson 和 Wang(2004)指出地表反照率随土壤湿度的增加而降低,且这种变化在土壤含水量较小时更加明显。在春季,农作物接近于成熟时植被叶绿素含量逐渐减小,含水量降低,地表反照率升高,当收割时,反照率达到最大,农作物播种、发芽和成长的过程中,地表反照率逐渐下降,当农作物生长最繁茂时,土壤含水量较大,地表反照率最低。ABD06 反照率产品很好地描述了这一过程,且整体上地面观测数据较为一致。表 4 是 GLASSABD 与地面观测数据在没有区分地表下垫面的情况下的对比结果。

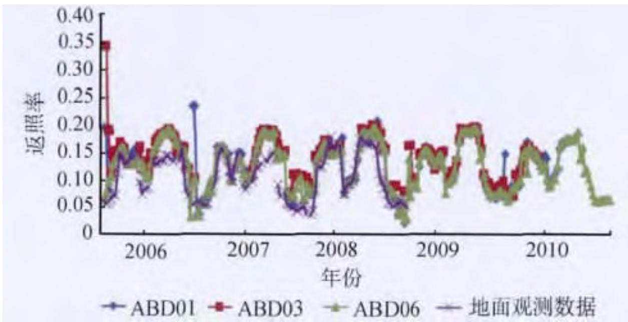

图7 ES-ES2 站点 2006 年—2010 年 5 年间 GLASSABD 与地面观测数据的时间序列图

表4 GLASSABD 与地面观测数据对比结果

数据类型	数据总量	系统偏差	RMSE	R^2
ABD01	4290	0.007	0.056	0.602
ABD03	3296	0.004	0.052	0.526
ABD06	5507	0.001	0.050	0.788

3.2 GLASSABD 与 MCD43B3 的对比分析

由于 NASA 发布的反照率产品 MCD43B3 时间分辨率也为 8 天,因此 GLASSABD 与 MCD43B3 进

行比较时数据处理的过程和 GLASSABD 与地面观测数据进行对比时一致。唯一的区别是没有对下垫面进行细分，而是将地表下垫面统称为植被。

3.2.1 各类产品数据统计与比较

在与 MCD43B3 进行比较时仍用上文提到的 24 个站点数据，时间跨度为 2006 年—2010 年，包括 ABD01 数据 4290 个，ABD03 数据 3296 个，ABD06 数据 5507 个，MCD43B3 数据 4696 个。可以看出，ABD06 几乎没有数据缺失，而 MCD43B3 数据缺失较多。仅从有效数据量考虑，ABD06 在时间序列上明显比 MCD43B3 更合适。图 8 给出了 GLASSABD 与 MCD43B3 的比较情况。

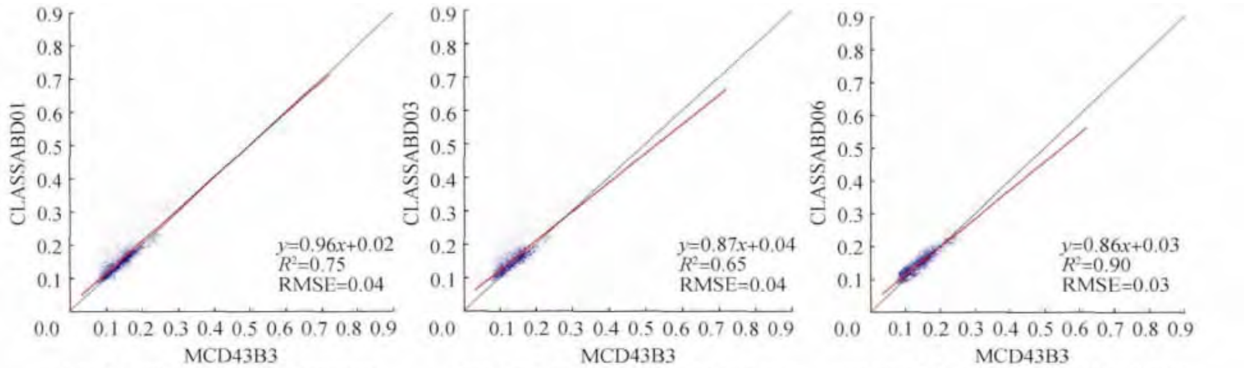

(a) GLASSABD01与MCD43B3的对比 (b) GLASSABD03与MCD43B3的对比 (c) GLASSABD06与MCD43B3的对比

图 8 GLASSABD 与 MCD43B3 对比图

3.2.2 对比结果分析

各种植被类型反照率产品 ABD01、ABD03、ABD06 与 MCD43B3 的对比结果表明，ABD06 反照率产品与 MCD43B3 的一致性最好，ABD01、ABD03 均存在数据缺失现象，且有一些突变点不能较好地与 MCD43B3 相吻合。ABD01 和 ABD03 中这些误差可能由大气校正误差、不同日期 MODIS 像元几何位置的偏差和算法本身的不确定性引起的，也可能是这些突变点符合实际情况但在作为 STF 算法输入数据时通过融合滤波被去掉，这就需要有更多的先验知识融入到生产过程中。经过以上长时间序列的验证，ABD06 数值上略大于 MCD43B3，相比于 ABD01 和 ABD03 更接近于 MCD43B3，但是 ABD01、ABD03 也达到了预期的效果。STF 算法适合生产长时间序列的反照率产品。表 5 为 GLASSABD 与 MCD43B3 比较结果汇总。

表 5 GLASSABD 与 MCD43B3 对比结果

数据类型	数据总量	系统偏差	RMSE	R^2
ABD01	4290	0.12	0.04	0.75
ABD03	3296	0.13	0.04	0.65
ABD06	5507	0.007	0.03	0.90

4 结 论

本文选取了 24 个地面观测站点，利用 2006 年—2010 年长时间序列的 AB1、AB2、STF 以及 MCD43B3 反照率产品和相应的地面观测数据进行对比分析，定量地验证 AB1、AB2 和 STF 3 种算法的反照率产品质量。大量数据的统计结果表明：AB1 和 AB2 算法反照率产品达到了预期的效果，满足了一定的精度要求（与地面观测站点数据对比 R^2 优于 0.5，RMSE 约为 0.05；与 MCD43B3 比较 R^2 优于 0.65，RMSE 优于 0.04）。作为滤波融合产品，STF 算法生产的反照率产品有效数据较多，在时间序列上比较连续，变化比较稳定。在与地面观测数据进行对比时发现 STF 算法表现出了一定优越性，它与地面观测数据符合最好，系统偏差接近 0.001，RMSE 优于 0.05，R^2 接近 0.8。与 MCD43B3 的对比结果表明：采用 STF 算法生产的 ABD06 与 MCD43B3 反照率产品拟合性最好，系统偏差优于 0.007，RMSE 接近 0.03，R^2 优于 0.9。大量验证结果还表明：3 种 GLASS 产品 80% 以上的数据与地面观测数据的偏差均能满足气候模式对反照率的精度要求（0.02—0.05）（Henderson-Sellers 和 Wilson，1983；Sellers，1993），但由于 AB1 与 AB2 在受云影响时存在数据缺失问题，因此使用 STF 生产的数据更适合作为全球变化研究的输入数据。

引起 AB1 和 AB2 算法反照率产品质量相对较差、数据量缺失较多的原因可能为大气校正的残余误差、不同日期 MODIS 像元几何位置的偏差，以及

AB1 和 AB2 算法的不确定性;同样,STF 算法也存在一定缺陷,比如滤波融合的时候有可能会滤掉一些符合实际情况但跳动较大的点,李小文等人(Li 等,1995)强调了先验知识在遥感反演中的重要性,要得到更高精度的反演值,就需要引入更多的先验知识。

参考文献(References)

Cescatti A, Marcolla B, Santhana Vannan S K, Pan J Y, Román M O, Yang X Y, Ciais P, Cook R B, Law B E and Matteucci G, Migliavacca M, Moors E, Richardson A D, Seufert G and Schaaf C B. 2012. Intercomparison of MODIS albedo retrievals and in situ measurements across the global FLUXNET network. Remote Sensing of Environment, 121: 323 - 334 [DOI: 10.1016/j.rse.2012.02.019]

Davidson A and Wang S S. 2004. The effects of sampling resolution on the surface albedos of dominant land cover types in the North American boreal region. Remote Sensing of Environment, 93(1/2): 211 - 224 [DOI: 10.1016/j.rse.2004.07.005]

Dickinson R E. 1995. Land processes in climate models. Remote Sensing of Environment, 51(1): 27 - 38 [DOI: 10.1016/0034 - 4257(94)00062 - R]

冯焱,冯海霞. 2012. 北京地区地表反照率 TM 数据反演与分析. 测绘科学,37(5): 164 - 166

Henderson-Sellers A and Wilson M F. 1983. Surface albedo data for climatic modeling. Reviews of Geophysics, 21(8): 1743 - 1778 [DOI: 10.1029/RG021i008p01743]

焦子锑,王锦地,谢里欧,张颢,阎广建,何立明,李小文. 2005. 地面和机载多角度观测数据的反照率反演及对 MODIS 反照率产品的初步验证. 遥感学报,9(1): 64 - 72

Li X W, Wang J D and Strahler A H. 1995. On utilization of *a priori* knowledge in inversion of remote sensing models. Science in China Series D (Earth Sciences), 41(6): 580 - 585 [DOI: 10.1007/BF02878739]

Liang S L. 2003. A direct algorithm for estimating land surface broadband albedos from MODIS imagery. IEEE Transactions on Geoscience and Remote Sensing, 41(1): 136 - 145 [DOI: 10.1109/TGRS.2002.807751]

Liang S L, Stroeve J and Box J E. 2005. Mapping daily snow/ice shortwave broadband albedo from Moderate Resolution Imaging Spectroradiometer (MODIS): the improved direct retrieval algorithm and validation with Greenland in situ measurement. Journal of Geophysical Research, 110(D10) [DOI: 10.1029/2004JD005493]

Liang S L, Zhao X, Liu S H, Yuan W P, Cheng X, Xiao Z Q, Zhang X T, Liu Q, Cheng J, Tang H R, Qu Y H, Bo Y C, Qu Y, Ren H Z, Yu K and Townshend J. 2013. A Long-term Global LAnd Surface Satellite (GLASS) data-set for environmental studies. International Journal of Digital Earth, [DOI: 10.1080/17538947.2013.805262]

Liu N F, Liu Q, Wang L Z, Liang S L, Wen J G, Qu Y and Liu S H. 2004. A statistics-based temporal filter algorithm to map spatiotemporally continuous shortwave albedo from MODIS data. Hydrology and Earth System Sciences, 17: 2121 - 2129 [DOI: 10.5194/hess-17-2121-2013]

Lucht W, Schaaf C B and Strahler A H. 2002. An algorithm for the retrieval of albedo from space using semiempirical BRDF models. IEEE Transactions on Geoscience and Remote Sensing, 38(2): 977 - 998 [DOI: 10.1109/36.841980]

Mason P and Reading B. 2005. Implementation Plan for the Global Observing System for Climate in Support of the UNFCCC. Geneva, Switzerland: WMO, IOC, UNEP, ICSU

Qu Y, Liu Q, Liang S, Wang L Z, Liu N F and Liu S H. 2013. Direct-estimation algorithm for mapping daily land-surface broadband albedo from MODIS data. IEEE Transactions on Geoscience and Re mote Sensing, (99): 1 [DOI: 10.1109/TGRS.2013.2245670]

Roujean J L, Leroy M and Deschamps P Y. 1992. A bidirectional reflectance model of the Earth's surface for the correction of remote sensing data. Journal of Geophysical Research, 97(D18): 20455 - 20468 [DOI: 10.1029/92JD01411]

Russell M J, Nunez M, Chladil M A, Valiente J A and Lopez-Baeza E. 1997. Conversion of nadir, narrowband reflectance in red and near-infrared channels to hemispherical surface albedo. Remote Sensing of Environment, 61(1): 16 - 23 [DOI: 10.1016/S0034 - 4257(96)00218 - 0]

Schaaf C B, Gao F, Strahler A H, Lucht W, Li X W, Tsang T, Strugnell N C, Zhang X Y, Jin Y F, Muller J P, Lewis P, Barnsley M J, Hobson P, Disney M, Roberts G, Dunderdale M, Doll C, D'Entremont R P, Hu B X, Liang S L, Privette J L and Roy D. 2002. First operational BRDF, albedo nadir reflectance products from MODIS. Remote Sensing of Environment, 83(1/2): 135 - 148 [DOI: 10.1016/s0034 - 4257(02)00091 - 3]

Sellers P J. 1993. Remote Sensing of Land Surface Climatology. NASA/GSFC Intematiorlal Satellite Land Surface C1inlatology Project Report. Greenbelt, Maryland: NASA Goddard Space Flight Center

Strahler A H, Lucht W, Schaaf C B, Tsang T, Gao F, Li X W, Muller J P, Lewis P and Barnsley M. 1999. MODIS BRDF/albedo product: algorithm theoretical basis document version 5.0. MODIS documentation

王艺,朱彬,刘煜,李维亮. 2011. 中国地区近 10 年地表反照率变化趋势. 气象科学,39(2): 147 - 155

Wanner W, Li X and Strahler A. 1995. On the derivation of kernels for kernel-driven models of bidirectional reflectance. Journal of Geophysical Research, 100(D10): 21077 - 21090 [DOI: 10.1029/95JD02371]

吴宏伊,童玲,陈云坪. 2012. 基于中国通量网的 MODIS 短波反照率验证与分析. 遥感技术与应用,27(5): 735 - 739

杨华,李小文,高峰. 2002. 新几何光学核驱动 BRDF 模型反演地表反照率的算法. 遥感学报,6(4): 246 - 251

余予,李扬云,童应祥,田红,陈洪滨. 2009. 寿县地区小麦和水稻田地表反照率观测分析. 气候与环境研究,14(6): 639 - 645